RESEARCH ARTICLE | FEBRUARY 23 2023

Charge transfer cross sections and transport coefficients of $^{39}K^+ - {}^{39}K$ and $^{41}K^+ - {}^{39}K$ at low-energy

Fouzia Bouchelaghem ; Moncef Bouledroua

AIP Advances 13, 025159 (2023)
https://doi.org/10.1063/5.0134588

Charge transfer cross sections and transport coefficients of $^{39}K^+ - {}^{39}K$ and $^{41}K^+ - {}^{39}K$ at low-energy

Cite as: AIP Advances 13, 025159 (2023); doi: 10.1063/5.0134588
Submitted: 17 November 2022 • Accepted: 1 February 2023 •
Published Online: 23 February 2023

Fouzia Bouchelaghem[1,a] and Moncef Bouledroua[2]

AFFILIATIONS

[1] Physics Department, Mohamed Boudiaf University, M'sila 28000, Algeria
[2] Physics Department, Badji Mokhtar University, B.P. 12, Annaba 23000, Algeria

[a] Author to whom correspondence should be addressed: fouziabouche@yahoo.fr and fouzia.bouchelaghem@univ-msila.dz

ABSTRACT

The transport coefficients, diffusion $D(T)$, and reduced mobility K_0 are calculated for systems $^{39}K^+ - {}^{39}K$ and $^{41}K^+ - {}^{39}K$ in a thermal range between 1 and 3000 K within the Chapman–Enskog approximation. This is preceded by a theoretical study of the collision of alkaline ions in their gases for low and intermediate energies in the range $10^{-14} \le E \le 10^{-3}$ (a.u.), and within this field, we calculate the interaction energy potentials and elastic and charge-transfer cross sections and discuss the isotopic effects in the $^{39}K^+ - {}^{39}K$ and $^{41}K^+ - {}^{39}K$ collisions.

I. INTRODUCTION

Charge-exchange collisions take place at high and low energies. At the time of collision, an electron is transferred from a neutral to an ion. If an ion collides with a neutral, charge-transfer produces a neutral and an ion,

$$A^+ + B \rightarrow A + B^+. \quad (1)$$

In this paper, we are interested in the analysis of the asymptotic theory of the charge-transfer process and certain thermodynamic properties of a monoatomic gas. The calculations we make in this study allow us to better understand the behavior of this process and consider the isotopic and symmetry effects, which is conducted in low and intermediate energies. We applied this study to the collision of alkaline ions in their gases such as $K^+ - K(4s)$ in their ground states, which are either *gerade* (g) or *ungerade* (u), namely, $^2\Sigma_g^+$ or $^2\Sigma_u^+$. We have focused on building the necessary interaction potentials, and this construction will be especially based on potential energy points theoretically determined very recently. In addition, the aim of this work is to quantify the phase shifts as a function of collision energy. Using the phase shifts obtained, we calculate the elastic and charge-transfer cross sections relating to systems $K^+ - K$, $^{39}K^+ - {}^{39}K$, and $^{41}K^+ - {}^{39}K$. We finish this work by computing the transport properties within the Chapman–Enskog approximation[1] for temperatures ranging from 1 to 3000 K.

Atomic units (a.u.) are used throughout this paper, unless otherwise stated.

II. INTERACTION POTENTIALS

The interaction potentials $V(R)$ between the atom and the ion are generally constructed in three main regions of distance: long, intermediate, and short regions. At intermediate distances, $R_1 \le R \le R_L$, where R_1 is the radius corresponding to the data of the first point and R_L is the last point. We adopted the *ab initio* values of the energies potential provided in Ref. 2, ranging from 5.0 to 50.0 Bohr radii. The short internuclear distances ($R \le 5.0$ Bohrs radii), which depend essentially on the overlap of electronic charge clouds between atomic nuclei and ionic nuclei, generate a repulsive interaction potential that can be expressed in the Born–Meyer analytical form as

$$V_{\text{rep}}(R) \sim W \exp(-wR). \quad (2)$$

W and w are the potential parameters,[3]

$$w = -\frac{1}{V(R)} \frac{dV(R)}{dR}\bigg|_{R=R_1}, \quad (3)$$

$$W = V(R)\exp(+wR)|_{R=R_1}. \quad (4)$$

For the internuclear distances ($R \geq 50.0$ Bohrs radii), the energy curve is generally called a *long-range* potential curve, and this potential is independent of such an overlap, depending rather on the correlation of electron motions caused by Coulomb effects. We write it using the following asymptotic formula:

$$V_{LR}(R) \sim V_{disp}(R) \mp V_{exch}(R), \quad (5)$$

where the − and + signs are used with the g and u potentials, respectively. The first term $V_{disp}(R)$ is the long-range dispersion potential function defined by the relationship

$$V_{disp}(R) = -\frac{C_4}{R^4} - \frac{C_6}{R^6} - \frac{C_8}{R^8}, \quad (6)$$

where the dispersion coefficients $C_4 = \frac{1}{2}\alpha_d$, $C_6 = \frac{1}{2}\alpha_q$, and $C_8 = \frac{1}{2}\alpha_o$ are correlated with the dipole α_d, quadrupole α_q, and octupole α_o polarizabilities of the neutral atom K(4s), respectively. In this work, for both K_2^+ molecular states, we utilized the measured value of the dipole polarizability, $\alpha_d = 287.6$, provided in Ref. 4. This α_d is very close to many other polarizabilities that have been generated, theoretically or experimentally, during the last decade, such as 289.1 given in Ref. 5, 289.3 given in Ref. 6, 290.2 given in Ref. 7, 290,33 given in Ref. 8, 292.8 given in Ref. 9, and 308.3 given in Ref. 10. We have further adopted the most recent quadrupole, $\alpha_q = 4.730 \times 10^3$, and octupole, $\alpha_o = 16.5 \times 10^4$, polarizabilities, as computed in Ref. 11. These results agree quite well with the multipolar polarizabilities $\alpha_q = 4.597 \times 10^3$ and $\alpha_o = 15.02 \times 10^4$ of Ref. 12 or $\alpha_q = 4.983 \times 10^3$ and $\alpha_o = 17.73 \times 10^4$ of Ref. 13, which in turn leads to standard mobility, also known as the *polarization* mobility, in the limit of zero-field strength and zero gas temperature,[14]

$$K_{pol} = 13.853(\alpha_d \mu)^{-\frac{1}{2}}. \quad (7)$$

μ is the reduced mass in atomic mass units, $\alpha_d = 42.57$ in Å^3, and K_{pol} is in cm^2 V^{-1}s^{-1}. The exchange interaction potentials of an ion with the parent atom were found using the treatment provided in Ref. 15 and take the form (in atomic units)

$$V_{exch}(R) = \frac{1}{2}\mathcal{A}^2 R^{2/\gamma - 1}\exp(-\gamma R). \quad (8)$$

Here, $\gamma = 0.769$, and $\mathcal{A} \simeq 0.598$.[15]

The K_2^+ potential energy curves thus constructed are shown in Fig. 1. The present *gerade* and *ungerade* curves are also compared with some data from the study by Rabli and McCarroll,[16] Johann *et al.*,[9] and Ilyabaev and Kaldor.[17] The constant parameters that appear in the form of short distances in Eq. (2) took the following values:

For $^2\Sigma_g^+$ potential, $W = 538.3$ a.u. and $w = 1.984$ a.u., and for $^2\Sigma_u^+$ potential, $W = 1.106$ a.u. and $w = 0.475$ a.u. The g and u equilibrium distances R_e and potential well depths D_e are displayed in Table I and compared with the published results. In this work, we found that $^2\Sigma_g^+$ potential has a well depth $D_e = 6687$ cm^{-1} corresponding to an equilibrium position $R_e = 4.477$ Å and that $^2\Sigma_u^+$ potential has a well depth of $D_e = 86.50$ cm^{-1} corresponding to an equilibrium position $R_e = 11.748$ Å. These values are very close to the results listed in the table.

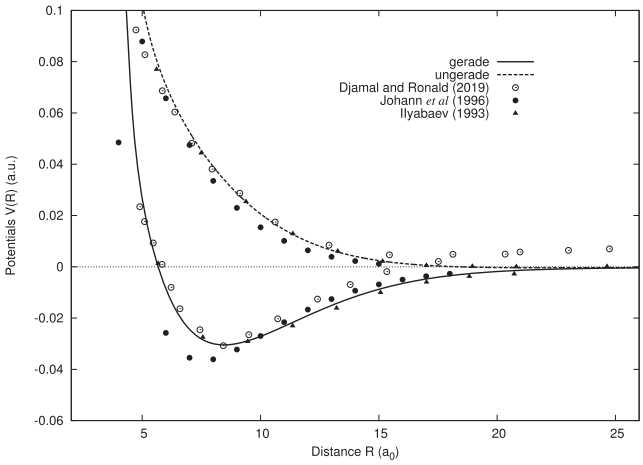

FIG. 1. Potential-energy curves of the gerade and ungerade $K^+ - K$ electronic states. The curves are compared with published data from the study by Djamal and McCarroll,[16] Johann *et al.*,[9] and Ilyabaev and Kaldor.[17]

Having appropriately determined the inter-atomic potential $V(R)$, it is now possible to numerically solve the radial wave equation

$$\left[\frac{d^2}{dR^2} + k^2 - 2\mu V(R) - \frac{l(l+1)}{R^2}\right]u_l(R) = 0. \quad (9)$$

The phase shifts η_l that we need here to completely describe the binary collisions are obtained after a numerical computation of the partial waves $u_l(R)$ used for each molecular state of the corresponding potential $V(R)$. This can be performed with the Numerov algorithm,[20] where the asymptotic form of $u_l(R)$ is required to have the behavior

$$u_l(R) \sim \sin\left(kR - \frac{l}{2}\pi + \eta_l\right).$$

For each kinetic moment orbital l and relative energy, $E = \hbar^2 k^2/2\,\mu$. In practice, the calculations of $\eta_l(E)$ are carried out for all energies

TABLE I. Potential characteristics compared to published results.

K_2^+ states	R_e (a_0)	$-D_e$ (a.u.)	References
$^2\Sigma_g^+$	8.46	0.304×10^{-1}	This work
	8.58	0.294×10^{-1}	10
	8.33	0.302×10^{-1}	16
	8.38	0.295×10^{-1}	18
	8.30	0.304×10^{-1}	19
$^2\Sigma_u^+$	22.20	0.394×10^{-3}	This work
	22.43	0.364×10^{-3}	10
	22.18	0.364×10^{-3}	16
	22.39	0.373×10^{-3}	18
	22.55	0.364×10^{-3}	19

between $E_{min} = 10^{-14}$ a.u. and $E_{max} = 10^{-3}$ a.u., with the maximum value of the kinetic moment orbital $l_{max} = 1000$. The calculations will be performed quantum mechanically at a certain value $l = l_{sc}$, beyond which the program is forced to use the approximate semi-classical given by the equation[3]

$$\eta_l^{g,u}(E) = \frac{\pi\mu^2 C_4}{2\hbar^4}\frac{E}{l^3}. \tag{10}$$

III. ELASTIC CROSS SECTION

At low energy, quantum effects become important. This then requires us to introduce the symmetry effects due to the identity colliding atoms and the spin of their nucleus into the calculations. However, first, we chose to perform the calculations without consideration of these quantum effects. Let's talk about systems containing non-identical atoms and ions.

A. Effect of symmetry and spin not included

Here, the calculations of the total elastic cross sections relative to both *gerade* and *ungerade* states are given by[21]

$$Q_{el}^{tot}(E) = \frac{1}{2}\left[Q_{el}^{g} + Q_{el}^{u}\right], \tag{11}$$

where

$$Q_{el}^{g,u}(E) = \frac{4\pi}{k^2}\sum_{l=0}^{\infty}(2l+1)\sin^2\left(\eta_l^{g,u}\right). \tag{12}$$

In their work, Côté and Dalgarno[3] demonstrated sodium collisions $Na^+ - Na$, and the semi-classical cross section is expressed by the relationship

$$Q_{el}(E) = \pi\left(\frac{\mu\alpha_d^2}{\hbar^2}\right)^{\frac{1}{3}}\left(1 + \frac{\pi^2}{16}\right)E^{-\frac{1}{3}}. \tag{13}$$

This expression is gleaned from a procedure developed entirely by Mott and Massey[22] and successfully applied to collisions between neutrals and neutral ions. For $K^+ - K$, this equation leads to the numerical result in atomic units,

$$Q_{el}(E) = 8.505 \times (10)^3 E^{-\frac{1}{3}}. \tag{14}$$

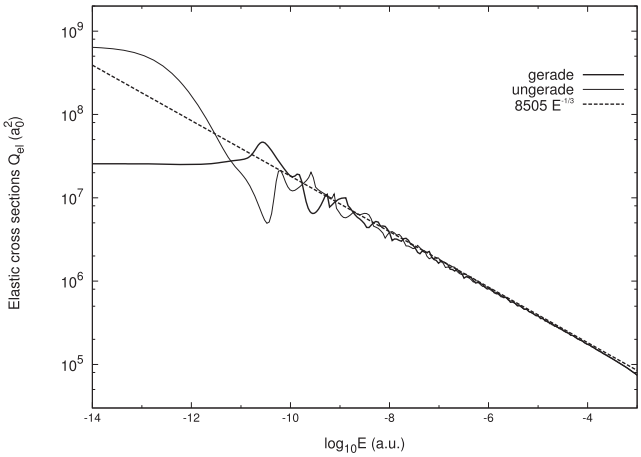

FIG. 2. Elastic g and u scattering cross sections Q_{el} (E) for K^+ ions scattered by atomic K. Dashed lines represent the semiclassical cross sections given in Eq. (14).

B. Effect of symmetry and spin included

Because of the identity of the nuclear fields, there are two possible modes of interaction between an atomic ion and its parent atom: one $V^+(R)$ symmetric in the nuclei and the other $V^-(R)$ antisymmetric.[23] This then requires that we introduce the symmetry effects and spin of their core into the calculations. In the case of Fermi–Dirac statistics, the elastic cross section Q_{el} for $^{39}K^+$ ions scattered by ^{39}K atoms with identical nuclei of spin $s = 3/2$ is given by[23,24]

$$Q_{el} = \frac{s}{2s+1}Q^+ + \frac{s+1}{2s+1}Q^-, \tag{15}$$

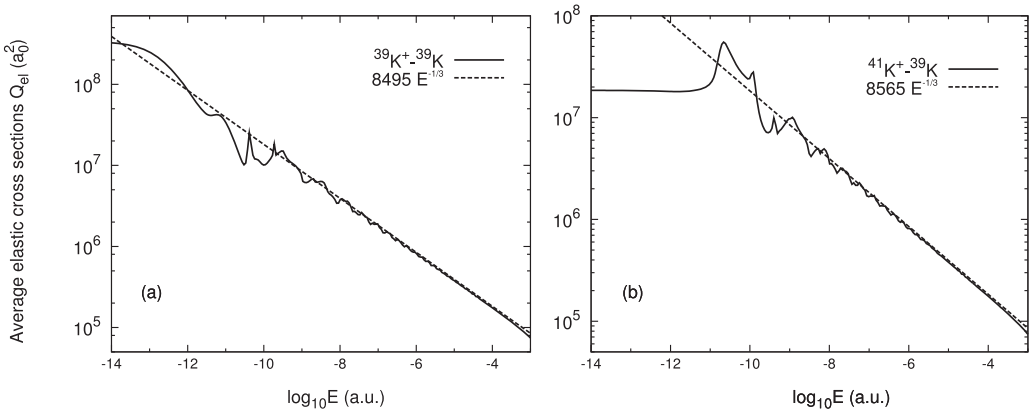

FIG. 3. Average elastic cross sections for both isotopes $^{+39}K - {}^{39}K$ and $^{+41}K - {}^{39}K$.

where

$$Q^{+} = \frac{4\pi}{k^2}\left[\sum_{l\,\text{even}}(2l+1)\sin^2\eta_l^g + \sum_{l\,\text{odd}}(2l+1)\sin^2\eta_l^u\right] \quad (16)$$

and

$$Q^{-} = \frac{4\pi}{k^2}\left[\sum_{l\,\text{odd}}(2l+1)\sin^2\eta_l^g + \sum_{l\,\text{even}}(2l+1)\sin^2\eta_l^u\right]. \quad (17)$$

Our cross-sectional data varying with energy for both states $^2\Sigma_g^+$ and $^2\Sigma_u^+$ of the $K^+ - K$ system are shown in Fig. 2, and the fit of numeric data given in Eq. (14) is also presented. Figure 3 shows the variation in the average section in the case of diffusion of $^{39}K^+$ and $^{41}K^+$ ions in a neutral gas ^{39}K. It shows in particular the importance of isotopic effects at low energies. Beyond the energy $E \approx 10^{-6}$ a.u., the average elastic cross sections of the two systems become almost similar, which demonstrates the collapse of the isotopic effects. It is noted that the cross elastic sections of the high energies fit the expression $Q_{\text{el}}(E) = C_{\text{el}}E^{-\frac{1}{3}}$, where $C_{\text{el}} = 8.495 \times 10^3$ for system $^{39}K^+ - {}^{39}K$ and $C_{\text{el}} = 8.565 \times 10^3$ for $^{41}K^+ - {}^{39}K$.

IV. CHARGE TRANSFER AND DIFFUSION CROSS SECTIONS

When a charged ion K^+ collides with an atom of the same species K, an electron can be transferred from the atom to the ion without affecting the internal energy of colliding particles. In this case, the cross section for charge-transfer is theoretically defined as[21]

$$Q_{ch} = \frac{\pi}{k^2}\sum_{l=0}^{\infty}(2l+1)\sin^2\left(\eta_l^g - \eta_l^u\right), \quad (18)$$

and the charge-transfer cross section varies approximately as the classical Langevin formula does for a polarization potential,[3]

$$Q_{\text{Langevin}} = \pi\sqrt{2\alpha_d}E^{-\frac{1}{2}}\ \text{a.u.} \quad (19)$$

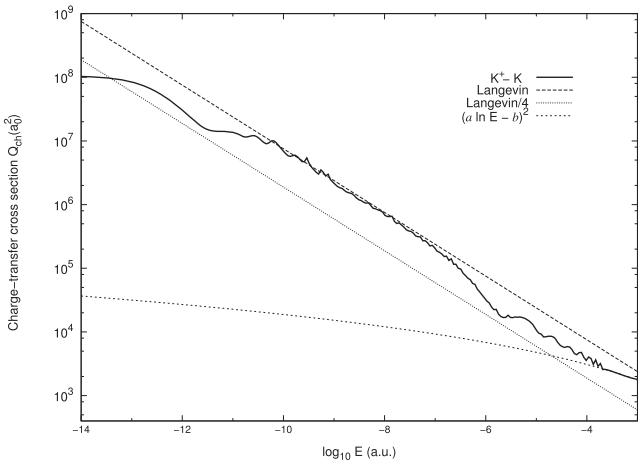

FIG. 4. K_2^+ charge-transfer cross sections and their behavior with energy. The limit at higher energies is given by Eq. (20). The classical Langevin cross sections Q_L and $Q_L/4$ are also presented.

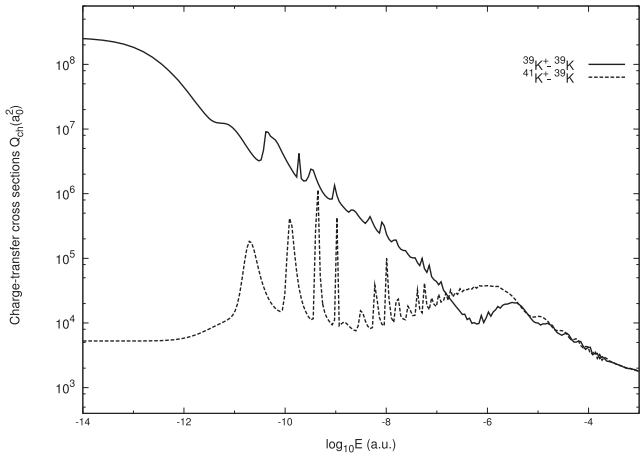

FIG. 5. Charge-transfer cross sections for both potassium isotopes.

In Fig. 4, we present our results over a wide range of energies calculated by Eq. (18). At lower energies, our cross sections are higher because of the polarization attraction force.[25] At high energies, the influence of the long-range attractive force tends to cancel, and the cross section is determined by the exponential decay of the difference between the potentials $^2\Sigma_g^+$ and $^2\Sigma_u^+$.[3] Figure 4 also shows that quantum Q_{ch} results fall over a wide range of energy, almost entirely in the interval $\left[\frac{1}{4}Q_L, Q_L\right]$, The same restriction range for the charge-transfer cross section was found in a previous study of the lithium system.[26] Above 10^{-3} a.u., the cross section varies approximately as[21,23]

$$Q_{ch} = (a\ln E - b)^2. \quad (20)$$

Here, $a = 5.90$ and $b = 1.15$ are constants that are dependent upon the collision system being studied, and E is expressed in a.u. Using the theoretical methods described above, our calculations could output the charge-transfer cross sections $Q_{ch} = 41.71 \times 10^{-15}$ cm^2 at

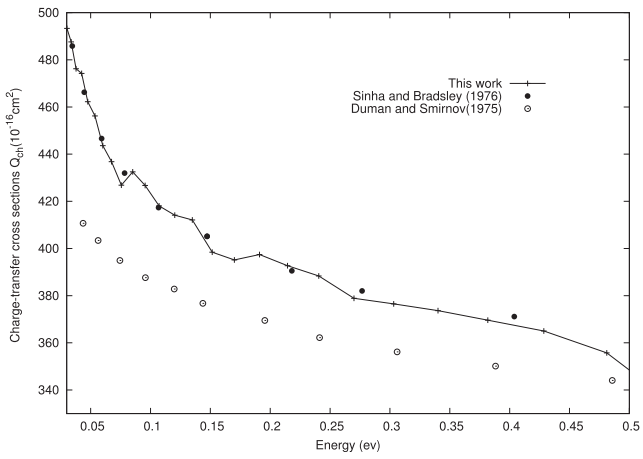

FIG. 6. Charge-transfer cross sections at low energies for standard K_2^+ compared with data from the study by Sinha and Bardsley[25] and Duman and Smirnov.[28]

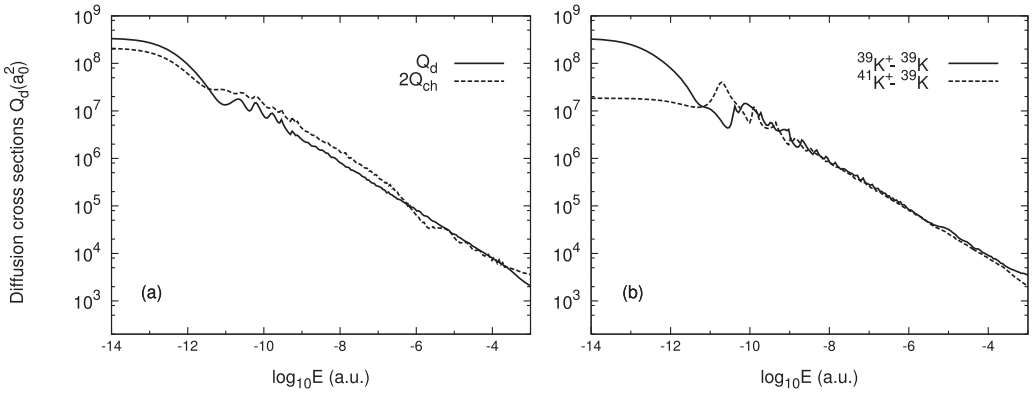

FIG. 7. Diffusion cross sections varying with energy. They are compared with $2Q_{ch}$ in (a) and determined for both lithium isotopes in (b).

energy $E = 0.1$ eV. For the same energy, the analytical relationship (20) leads to the values 42.03×10^{-15} cm^2. These data agree quite well with the value 40×10^{-15} cm^2 in Ref. 27. In addition, the charge transfer cross sections for systems $^{39}K^+ - {}^{39}K$ and $^{41}K^+ - {}^{39}K$ are shown in Fig. 5. We can notice that the isotopic effect appeared for the collision energy $E \leq 10^{-4}$ a.u. and both colliding species exhibit orbiting resonances that occur at almost the same energies. However, as the energy increases, the two curves seem to coincide with the form (20). For comparison, in Fig. 6, we present the charge transfer cross sections calculated at low energies and compared with data by Sinha and Bradsley[25] and Duman and Smirnov.[28] Below $E = 0.25$ eV, small oscillations are apparent, caused by the interference between each pair of the *g* and *u* potential–energy curves.[29] The difference between the *gerade* and *ungerade* phase shifts for small partial waves shows significant variations with energy in the region of the potential well, but the curves become practically linear above the energy 0.25 eV.

The diffusion cross section in the case where symmetry and spin effects not included takes the form[22,23]

$$Q_1(E) = \frac{4\pi}{k^2}\sum_{l=0}^{\infty}(l+1)\sin^2(\eta_{l+1} - \eta_l). \tag{21}$$

For fermion, the diffusion cross section for an ion in its parent species is given by[23]

$$Q_1(E) = \frac{s}{2s+1}Q_1^+ + \frac{s+1}{2s+1}Q_1^-, \tag{22}$$

where

$$Q_1^+ = \frac{4\pi}{k^2}\left[\sum_{l=even}^{\infty}(l+1)\sin^2(\eta_l^g - \eta_{l+1}^u) + \sum_{l=odd}^{\infty}(l+1)\sin^2(\eta_l^u - \eta_{l+1}^g)\right] \tag{23}$$

and

$$Q_1^- = \frac{4\pi}{k^2}\left[\sum_{l=even}^{\infty}(l+1)\sin^2(\eta^u - \eta_{l+1}^g) + \sum_{l=odd}^{\infty}(l+1)\sin^2(\eta_l^g - \eta_{l+1}^u)\right]. \tag{24}$$

For large l, $\eta_l^{g,u} \simeq \eta_{l+1}^{g,u}$. With $Q_1(E) = Q_d$, we find according to what was mentioned in Ref. 23,

$$Q_d \simeq 2Q_{ch}. \tag{25}$$

In Figs. 7(a) and 7(b), we present the variations in the diffusion cross sections $Q_1(E)$ of potassium and the two isotopes as a function of the collision energy and compare it to twice the charge-transfer cross section. The agreement is closer, and we also note that the isotope effect is especially important at very low energies.

V. MOBILITY AND DIFFUSION COEFFICIENTS

Using the diffusion cross section, we can calculate the ion mobility. The mobility of an ion is given by[23]

$$K = \frac{eD}{k_B T}, \tag{26}$$

where e is the ionic charge, k_B is Boltzmann's constant, and $D = D(T)$ is the temperature-dependent coefficient of diffusion. Usually, to facilitate the comparison of data, the mobility of the ions is given as the *reduced* mobility,

$$K_0 = \frac{P}{760}\frac{273.15}{T}K, \tag{27}$$

with P being the gas pressure in torrs, T in Kelvins, and K and K_0 in cm^2 V^{-1}s^{-1}. The diffusion coefficient D is determined by using the Chapman–Enskog model for binary systems, which considers low-density ions of density n_1 diffusing in a neutral gas of density n_2.[23] If μ denotes the reduced mass of the colliding ion-neutral species, the diffusion coefficient is

$$D(T) = \frac{3k_B T}{16\mu(n_1+n_2)}\frac{1+\varepsilon_0}{\Omega^{(1,1)}(T)}. \tag{28}$$

TABLE II. Diffusion coefficients and correction factors. Numbers in square brackets are powers of 10.

	K^+ in K		$^{39}K^+$ in ^{39}Li		$^{41}K^+$ in ^{39}K	
Temperature T (K)	$D\ (cm^2s^{-1})$	ε_0	$D\ (cm^2s^{-1})$	ε_0	$D\ (cm^2s^{-1})$	ε_0
1	0.46[−4]	0.083	0.40[−4]	0.073	0.46[−4]	0.088
50	2.54[−3]	0.092	1.95[−3]	0.077	2.52[−3]	0.099
100	0.53[−2]	0.096	0.35[−2]	0.064	0.53[−2]	0.103
200	0.10[−1]	0.089	0.57[−2]	0.050	0.10[−1]	0.095
300	0.15[−1]	0.081	0.75[−2]	0.045	0.15[−1]	0.087
400	0.20[−1]	0.079	0.92[−2]	0.046	0.20[−1]	0.085
500	0.25[−1]	0.084	1.11[−2]	0.053	0.25[−1]	0.090
600	0.31[−1]	0.092	1.34[−2]	0.065	0.31[−1]	0.099
700	0.38[−1]	0.104	1.61[−2]	0.080	0.38[−1]	0.112
800	0.47[−1]	0.118	1.95[−2]	0.097	0.47[−1]	0.127
900	0.57[−1]	0.133	0.23[−1]	0.115	0.57[−1]	0.143
1000	0.69[−1]	0.148	0.28[−1]	0.133	0.69[−1]	0.159
1500	1.62[−1]	0.213	0.63[−1]	0.209	1.61[−1]	0.228
2000	0.32	0.259	0.12	0.261	0.32	0.277
3000	0.98	0.316	0.37	0.320	0.97	0.337

Here, $k = \sqrt{2\,\mu E}$ is the wave number, and $\Omega^{(1,1)}$ is the *diffusion* collision integral, which can be deduced from a more general formula,

$$\Omega^{(p,q)}(T) = \sqrt{\frac{k_B T}{2\pi\mu}} \int_0^\infty Q_p(x) x^{2q+3} \exp(-x^2) dx. \tag{29}$$

For the case of dilute gases, that is, $n_1 \ll n_2$, the correction factor ε_0 in Eq. (28) is expressed by Chapman and Cowling[30] as

$$\varepsilon_0 = \frac{5(C-1)^2}{5 - 4B + 8A(M_2/M_1) + 6(M_2/M_1)^2}, \tag{30}$$

where M_1 is the mass of the atomic species diffusing in the buffer gas made of the atomic species of mass M_2. The parameters A, B, and C are the ratios,

$$A = \frac{\Omega^{(2,2)}}{5\Omega^{(1,1)}}, \tag{31}$$

$$B = \frac{5\Omega^{(1,2)} - \Omega^{(1,3)}}{5\Omega^{(1,1)}}, \tag{32}$$

$$C = \frac{2\Omega^{(1,2)}}{5\Omega^{(1,1)}}. \tag{33}$$

In Eq. (31), the *viscosity* collision integral $\Omega^{(2,2)}$ is calculated from the viscosity cross section $Q_{p=2}$, which is defined by the summation[22]

$$Q_2(E) = \frac{4\pi}{k^2} \sum_{l=0}^{\infty} \frac{(l+1)(l+2)}{2l+3} \sin^2(\eta_{l+2} - \eta_l). \tag{34}$$

The values of $D(T)$ presented in Table II include the correction factor ε_0 in expression (28). Our values are compared specially in system $^{39}K^+ - {}^{39}K$ with those obtained by Smirnove. As an example, we found, in particular, the values 0.0075 and 0.019 $cm^2\ s^{-1}$ at T = 300 and 800 K, respectively. These data are closely comparable with 0.0074 and 0.014 $cm^2\ s^{-1}$ of Ref. 31. We also present the results of the calculation of the correction factor with a temperature between 1 and 3000 K. We note that the correction factor ε_0 for K^+ in K equals 0.083 at 1 K and passes through a maximum value of 0.31 at 3000 K, the correction factor for $^{39}K^+$ in ^{39}K is 0.073 at 1 K temperature, at 3000 K, ε_0 takes a value of 0.32, and for $^{41}K^+$ in ^{39}K, the correction factor equals 0.085 at 1 K temperature and passes a maximum value of 0.33 at 3000 K. The correction factor depends on the ratios of elastic cross sections and is relatively insensitive to the interaction potentials.[32]

We calculated the *reduced* mobility of K^+ ions in the parent atom gas K in a wide temperature range T = 1 – 3000 K from Eq. (27) using the diffusion coefficients calculated in our work. Table III presents the calculated of *reduced* mobilities under standard conditions (P_0 = 760 Torrs and gas temperature = 0 °C). The measurement was performed at gas pressure P = 101.325 kPa. We note at T = 1 K that in K^+ in K, $^{39}K^+$ in ^{39}K, and $^{41}K^+$ in ^{39}K systems, the *reduced* mobilities take values of 0.536, 0.470, and 0.537 ($cm^2\ V^{-1}s^{-1}$), respectively, and these values are approximately constants in the range of temperature between 1 and 100 K. Above 100 K, the reduced mobilities will ultimately increase. As can be noted in the deviation in values of *reduced* mobility of the $^{39}K_2^+$ system, this difference is due to the spin and symmetry effect. At a temperature of 300 K, the reduced mobility takes the value of 0.29 $cm^2\ V^{-1}s^{-1}$ in system $^{39}K^+ - {}^{39}K$, which is close to the value at 0.29 $cm^2\ V^{-1}s^{-1}$ in Ref. 31. The fact that K_0 depends on T indicates that the interaction of K^+ in the parent gas atom K is not a pure polarization interaction since for a pure polarization interaction, the reduced mobility is independent of temperature and can be expressed as Eq. (7). With this expression, we find that the K_{pol} of the K^+ in K is 0.480, which is the same as that found in Ref. 33. The K_{pol}

TABLE III. Reduced mobility K_0, varying with temperature.

Temperature T (K)	K^+ in K	$^{39}K^+$ in ^{39}Li	$^{41}K^+$ in ^{39}K
		K_0 $(cm^2\ V^{-1}s^{-1})$	
1	0.536	0.470	0.537
50	0.589	0.454	0.586
100	0.623	0.407	0.620
200	0.619	0.335	0.616
300	0.599	0.292	0.596
400	0.588	0.268	0.584
500	0.592	0.259	0.588
600	0.612	0.259	0.608
700	0.645	0.268	0.641
800	0.690	0.282	0.686
900	0.746	0.302	0.741
1000	0.810	0.325	0.805
1500	1.257	0.492	1.249
2000	1.900	0.735	1.888
3000	3.810	1.460	3.786

of $^{39}K^+$ in ^{39}K and of $^{41}K^+$ in ^{39}K is 0.481 and 0.475 $(cm^2\ V^{-1}s^{-1})$, respectively.

VI. CONCLUSION

In conclusion, our work is based on the quantum study of collisions between atoms and ions which was based on the case of the collision of alkaline ions in their gases. After a brief presentation of quantum collision theory, we built the potentials for $K^+ - K$ in the *gerade* and *ungerade* states. These potentials were used to solve the numerical equation of radial waves and, consequently, to numerically determine that for any energy E and all orbital angular momentum l, the phase shifts allow the various sections to be expressed efficiently by thermophysical spectroscopy. We also treated the variations in elastic and charge transfer sections in the quantum and semi-classical case. Under the model developed by Chapman and Enskog for sufficiently diluted gases, we have examined the properties of diffusion and reduced mobility of potassium K in detail. In the first step, we neglected the effects of symmetry and spin due to the identity of the colliding atoms. In this framework, we studied diffusion coefficient $D(T)$ changes with temperature in a wide range of 1–3000 K. In the second step, we then included the effects of symmetry and nuclear spins in the model, and we found that the symmetry of the atoms affects the change in the diffusion coefficient, especially at lower temperature. We therefore used the diffusion coefficient for calculating the *reduced* mobility in the same range of temperature. At low temperature, the *reduced* mobility is almost constant, and the increase in temperature gives growth in the values of reduced mobility.

ACKNOWLEDGMENTS

The author is very grateful to the Algerian *Ministry of Higher Education and Scientific Research* for support.

AUTHOR DECLARATIONS

Conflict of Interest

The authors have no conflicts to disclose.

Author Contributions

Fouzia Bouchelaghem: Methodology (equal); Writing – original draft (lead). **Moncef Bouledroua**: Methodology (equal).

DATA AVAILABILITY

The data that support the findings of this study are available from the corresponding author upon reasonable request.

REFERENCES

[1] L. E. Reichl, *A Modern Course in Statistical Physics* (University of Texas Press,Austin, 1984).
[2] A. Jraij, A. R. Allouche, S. Magnier, and M. Aubert-Frecon, Can. J. Phys. **86**, 1409–1415 (2008).
[3] R. Côté and A. Dalgarno, Phys. Rev. A **62**, 012709 (2000).
[4] E.-A. Reinsch and W. Meyer, Phys. Rev. A **14**, 915 (1976).
[5] J. Mitroy, M. S. Safronova, and C. W. Clark, J. Phys. B: At., Mol. Opt. Phys. **43**, 202001 (2010).
[6] U. I. Safronova and M. S. Safronova, Phys. Rev. A **78**, 052504 (2008).
[7] B. Gao, Phys. Rev. Lett. **104**, 213201 (2010).
[8] R. M. Sternheimer, Phys. Rev. **183**, 112 (1969).
[9] C. Johann, S. H. Patil, K. T. Tang, and J. P. Toennies, Chem. Phys. Lett. **295**, 158–166 (1998).
[10] H. Berriche, C. Ghanmi, M. Farjallah, and H. Bouzouita, J. Comput. Methods Sci. Eng. **8**, 297–318(2008).
[11] S. H. Patil and K. T. Tang, Chem. Phys. Lett. **295**, 152 (1998).
[12] J. M. Standard and P. R. Certain, J. Chem. Phys. **83**, 3002 (1985).
[13] S. G. Porsev and A. Derevianko, J. Chem. Phys. **119**, 844 (2003).
[14] G. A. Eiceman and Z. Karpas, *Ion Mobility Spectrometry*, 2nd ed. (CRC Press, Abingdon-on-Thames (Royaume-Uni), 2005).
[15] T. C. Scott, M. Aubert-Frécon, G. Hadinger, D. Andrae, J. Grotendorst, and J. D. Morgan, J. Phys. B: At., Mol. Opt. Phys. **37**, 4451 (2004).
[16] D. Rabli and R. McCarroll, Chem. Phys. Lett. **723**, 82–88 (2019).
[17] E. Ilyabaev and U. Kaldor, J. Chem. Phys. **98**, 7126 (1993).
[18] P. Skupin, M. Musiał, and S. A. Kucharski, J. Phys. Chem. A **121**, 1480–1486 (2017).
[19] S. Magnier and M. Aubert-Frécon, J. Quant. Spectrosc. Radiat. Transfer **78**, 217–225 (2003).
[20] B. Numerov, "Publ. Observatoire central astrophys," Russ **2**, 188 (1933).
[21] E. W. McDaniel, *Collision Phenomena in Ionized Gases*, Series in Plasma Physics (Wiley, New York, 1964).
[22] N. F. Mott and H. S. W. Massey, *The Theory of Atomic Collisions* (Oxford University Press, Oxford, 1966).
[23] A. Dalgarno, M. R. C. McDowell, and A. Williams, Philos. Trans. R. Soc. London, Ser. A **250**, 411 (1958).
[24] E. A. Mason and E. W. McDaniel, *Transport Properties of Ions in Gases* (Wiley and Sons Inc., New York, 1988).
[25] S. Sinha and J. N. Bardsley, "Symmetric charge transfer in low-energy ion atom collisions," Phys. Rev. A **14**, 104–113 (1976).
[26] F. Bouchelaghem and M. Bouledroua, J. Phys. Chem. Chem. Phys **16**, 1875–1882 (2014).

[27] B. M. Smirnov, Phys. Scr. **61**, 595 (2000).
[28] E. L. Duman and B. M. Smirnov, Sov. Phys. Tech. Phys. **15**, 61 (1970).
[29] J. A. S. Barata and C. A. N. Conde, IEEE Trans. Nucl. Sci. **52**, 2889 (2005).
[30] S. Chapman and T. G. Cowling, *Mathematical Theory of Non Uniform Gases* (Cambridge University Press, Cambridge, 1939).
[31] B. M. Smirnov, in *Reviews of Plasma Physics*, edited by V. D. Shafranov (Kluwer Academic/Plenum Publishers, New York, 2003), Vol. 23.
[32] H.-K. Chung and A. Dalgarno, Phys. Rev. A **66**, 012712 (2002).
[33] R. I. Golyatina, S. A. Maiorov, and G. B. Raghimkhanov, Phys. Sci. Technol. **5**, 83–89 (2018).